

Geostatistical Simulation for the Assessment of Regional Soil Pollution

Marc Van Meirvenne, Tariku Meklit

Department of Soil Management, Ghent University, Coupure 653, 9000 Ghent, Belgium

Regional scale inventories of heavy metal concentrations in soil increasingly are being done to evaluate their global patterns of variation. Sometimes these global pattern evaluations reveal information that is not identified by more detailed studies. Geostatistical methods, such as stochastic simulation, have not yet been used routinely for this purpose in spite of their potential. To investigate such a use of geostatistical methods, we analyzed a data set of 14,674 copper and 12,441 cadmium observations in the topsoil of Flanders, Belgium, covering 13,522 km². Outliers were identified and removed, and the distributions were spatially declustered. Copper was analyzed using sequential Gaussian simulation, whereas for cadmium we used sequential indicator simulation because of the large proportion (43%) of censored data. We complemented maps of the estimated values with maps of the probability of exceeding a critical sanitation threshold for agricultural land use. These sets of maps allowed the identification of regional patterns of increased metal concentrations and provided insight into their potential causes. Mostly areas with known industrial activities (such as lead and zinc smelters) could be delineated, but the effects of shells fired during the First World War were also identified.

Introduction

There is an increasing interest in regional studies of critical soil constituents, such as heavy metals, with the aims of examining their spatial distribution and of identifying the links with factors such as parent material, land use, or other human activities. This often involves large multivariate data sets that cover extensive areas. For example, Rawlins, Webster, and Lister (2003) investigated 13 elements determined at 4609 sites in eastern England (over about 10,000 km²) and found clear evidence of a relation between the geological structures and some chemical elements like magnesium and aluminum. Zhang et al. (2005) analyzed 48,544 samples (which were resampled to 16,511 locations), assayed for 27 elements, distributed across most of the conterminous United States. Two aims of such studies

Correspondence: Marc Van Meirvenne, Department of Soil Management, Coupure 653, 9000 Gent, Belgium
e-mail: marc.vanmeirvenne@ugent.be

Submitted: July 10, 2008. Revised version accepted: March 16, 2009.

are to characterize geochemical background values and to identify areas where concentrations are elevated. However, geochemical background values are difficult to define (Reimann and Garrett 2005) and consequently so are the threshold values used to identify contaminated or polluted soil. In Belgium, the Flemish government published official reference threshold values for background concentrations of several heavy metals in soil (Vlaamse-Gemeenschap 1996). For copper (Cu) this value is 17 mg kg^{-1} for a standard soil (defined as containing 10% clay and 2% organic matter), and for cadmium (Cd) it is 0.8 mg kg^{-1} . This is confirmed by the geochemical atlas of Europe (Salminen et al. 2005), which indicates, for example, a Cu baseline concentration in the topsoil of Flanders that fluctuates around 17.5 mg kg^{-1} . Although natural causes for increased concentrations can occur in soil weathered in situ, in Flanders concentrations above these official thresholds are considered to be human-induced contamination. Industrial activities are the most documented source of elevated concentrations of heavy metals in soils (Van Meirvenne and Goovaerts 2001; Papritz et al. 2005; Rawlins et al. 2006).

Our research focuses on the application of geostatistical simulation for the regional evaluation of topsoil concentrations of Cu and Cd over the entire area of Flanders, which covers $13,522 \text{ km}^2$. Studies covering smaller areas within Flanders have already been conducted, but maps of the spatial distribution over the entire region have not yet been available. Because of multiple sources of pollution, complex patterns and interactions can be expected that have not been identified in studies over smaller areas, and geostatistics has not been used for such purposes. Therefore, the objectives of this article are (1) to map geostatistically the regional patterns of topsoil Cu and Cd, (2) to delineate areas with a high probability of exceeding critical sanitation thresholds, and (3) to determine the potential sources responsible for the identified patterns.

Materials and methods

Study area and data

The study area covers the entire region of Flanders, which is the northern part of Belgium. The soil is dominantly developed in eolian sediments of the Holocene and Pleistocene ages (Van Meirvenne and Van Cleemput 2005). The northern part of the region is dominated by an acidic, humus-rich, sandy soil with a pH ranging between 3.8 and 7.6, with an average of 5.5. The central part of the region has a large area covered with sandy loam soil with an average pH of 6.1, ranging from 3.9 to 7.8. Wind-transported loess was deposited in the southern parts, resulting in loamy and silty textures with an average pH of 6.5, ranging from 4.4 to 8.0 (De Temmerman et al. 2003), depending on the degree of decalcification of the loess.

The data for Cu and Cd used in this study were received from the Public Waste Agency of Flanders (OVAM), the regulatory institute responsible for waste management and soil remediation in Flanders. These data were collected between 1988 and 2005 and represent a collection of many investigations, usually in the frame-

work of a soil sanitation study. OVAM prescribes the sampling and analytical procedures, so they can be expected to be reasonably homogeneous for the data set.

Each measurement was located by its geographical coordinates, upper and lower sampling depth, and sampling date. Because some samples had identical coordinates and variations in sampling depth, the data had to be screened carefully. In cases of multiple measurements at the same location, the most recent one was retained. Such measurements can result from sampling before and after remediation activities. In this study, we targeted the top 50 cm of the soil profile. The vertical distribution of Cu and Cd within the topsoil can be assumed to be reasonably uniform because of agricultural and other land preparation activities. When there were multiple samples within the top 50 cm, a depth-weighted average value was calculated using the depth intervals as weights.

The analytical procedure for total Cu and Cd analysis involves microwave destruction of 0.5 g of the air dry fine-earth fraction (<2 mm) of soil with 6 ml 37% hydrogen chloride, 2 ml 65% nitric acid, and 2 ml 40% hydrogen fluoride. In the resultant solution, metals were analyzed by either ICP-AES or graphite furnace atomic absorption spectrometry.

Geostatistical techniques

One of our aims in this study was to delineate areas with a high probability of exceeding critical sanitation thresholds; therefore, we needed a method that could provide a model of uncertainty rather than a prediction of the most likely value. The geostatistical toolbox offers several methods designed specifically to provide this information: indicator kriging, probability kriging, disjunctive kriging, stochastic simulation, and Bayesian maximum entropy. The reader is referred to standard geostatistics books for more detail on these methods (e.g., Goovaerts 1997; Chilès and Delfiner 1999; Christakos 2000; Webster and Oliver 2007).

In this research we used two types of stochastic simulation rather than kriging because it enabled us to obtain a model of the local uncertainty in a straightforward way. Moreover, the simulated realizations contain some desirable characteristics, such as a better reproduction of the spatial structure and distribution of the sample data, including patterns of spatial continuity if present in the data. Methods of kriging focus on providing the best estimate of a property at every location, but the resulting map shows less variation than the original data. Goovaerts (2000) describes in detail the differences in the objectives of estimation and simulation.

Stochastic simulation

Stochastic simulation draws multiple realizations of the spatial distribution based on the random function model of a variable. These realizations are created in such a way that they reproduce the general statistical characteristics of our sample distribution. With multiple realizations, we can derive a conditional cumulative distribution function (CCDF) of possible values at each location. These CCDFs can then be investigated by extracting several parameters (like the conditional mean or variance) or by evaluating the probability of exceeding a critical threshold value.

The construction of the CCDFs can be obtained through either a multi-Gaussian random model or an indicator approach (Goovaerts 2001). These two different ways of building the CCDF are demonstrated further by using two variants of stochastic simulations: sequential Gaussian simulation (SGS) and sequential indicator simulation (SIS). For both methods we used the GSLIB software (Deutsch and Journel 1998).

SGS

The SGS algorithm generates multiple realizations by following a number of consecutive steps; a flowchart of the SGS procedure is given in Fagroud and Van Meirvenne (2002). Because most environmental data do not follow a Gaussian distribution, transformation to a normal distribution is generally required (note that this condition is not necessary with kriging algorithms). We used a normal score transformation (equation [1]) to ensure that the global histogram would have a standardized Gaussian distribution:

$$y(\mathbf{x}_\alpha) = \phi(z(\mathbf{x}_\alpha)) \tag{1}$$

where $y(\mathbf{x}_\alpha)$ are the normal scores, $\phi(\cdot)$ is a normal score transformation function, $z(\mathbf{x}_\alpha)$ are the original data, \mathbf{x}_α is a location vector ($\alpha = 1, \dots, N$), and N is the number of available data (Goovaerts 1997; Deutsch and Journel 1998). Next, the variogram $\gamma(\mathbf{h})$ of the normal scores was calculated and modeled, and simulations of the normal scores were done at the nodes of a regular grid (500 m apart), visiting each location \mathbf{x}_0 along a predefined random path.

At every \mathbf{x}_0 , estimates of both the expected value and its prediction variance were produced by simple kriging (kriging with a known mean) using the model parameters of the normal score variogram, the data (minimally three and maximally 16 data), and previously simulated nodes (we used no more than 12 previously simulated nodes) within the kriging neighborhood. Using these estimates, we created a Gaussian distribution from which a value was drawn randomly: the simulated value for \mathbf{x}_0 . This continued until all locations had been visited, which represented one simulated image. By repeating the procedure, 500 simulated images were generated (generally believed to be sufficient; see Chilès and Delfiner 1999).

The results were back-transformed to the original scale of measurement of the variable by applying the inverse of the normal score transform $\phi(\cdot)$ to the simulated y values. At every location \mathbf{x}_0 , a CCDF of that node was constructed from the 500 values from the 500 realizations. This CCDF was used to determine the expected value at each location according to the following theoretical equation:

$$z_E^*(\mathbf{x}_0) = \int_{-\infty}^{+\infty} z dF(\mathbf{x}_0; z|(n)) \tag{2}$$

where $z_E^*(\mathbf{x}_0)$ is the estimated value and $F(\mathbf{x}_0; z|(n))$ is the CCDF at \mathbf{x}_0 conditioned to the n neighboring data. In practice, because we possess only a limited number of

realizations, this theoretical estimator is calculated as a simple averaging. The CCDF also enables the probability of exceeding a critical threshold, z_c , to be obtained:

$$\text{Prob}(Z(\mathbf{x}_0) > z_c) = 1 - F(\mathbf{x}_0; z_c | (n)) \tag{3}$$

To facilitate decision support, probability maps are often sorted into a few classes. We used three classes to represent low, medium, and high levels of confidence. The boundaries between these classes are a matter of choice; we used the lower and upper quartiles, that is, 0.25 and 0.75, to represent the lower and upper levels of confidence. The medium probabilities (i.e., 0.25–0.75) are the most uncertain to support decision making. Areas that fall into this class require additional investigation before a more reliable assessment can be made about the level of contamination.

SIS

The normal score transformation used in SGS can become problematic if there are large proportions of equal data (e.g., zeroes) or, in the case of censored data, data below an analytical threshold. This type of discontinuous data distribution prevents a transformation to normal scores. In such situations, converting the data into indicator values offers a solution, which then calls for SIS.

SIS is a nonparametric method of simulation based on an indicator coding of the values (Goovaerts, Webster, and Dubois 1997). It starts with the selection of K threshold values, z_k , used for the indicator coding according to

$$i(\mathbf{x}_\alpha; z_k) = \begin{cases} 1 & \text{if } z(\mathbf{x}_\alpha) \leq z_k \\ 0 & \text{otherwise} \end{cases} \quad k = 1, 2, \dots, K \tag{4}$$

where $i(\mathbf{x}_\alpha; z_k)$ is the indicator of observation $z(\mathbf{x}_\alpha)$ according to threshold z_k . Because there are K thresholds, every observation is converted into a vector of K indicators. After coding the data into indicators, an indicator variogram, $\gamma_I(\mathbf{h}; z_k)$, is calculated for each threshold and modeled.

The simulation follows a similar sequential procedure as in SGS, but indicator values, rather than normal scores, are simulated. At every location \mathbf{x}_0 , the K -simulated indicator values were used to build a distribution function from the ordinary indicator kriging estimates, which is for threshold z_k :

$$[F(\mathbf{x}_0; z_k | (n))]^* = [i(\mathbf{x}_0; z_k)]^* = \sum_{\alpha=1}^{n(\mathbf{x}_0)} \lambda_\alpha(z_k) \cdot i(\mathbf{x}_\alpha; z_k) \tag{5}$$

The weights $\lambda_\alpha(z_k)$ were obtained by solving the ordinary indicator kriging system. A random value was drawn from this distribution function and attributed to the grid node, after which the sequential procedure continued with the next grid node until all nodes had been visited. This was repeated 500 times so that at every \mathbf{x}_0 the CCDF of that node could be constructed from the values obtained from the realizations. However, generally, because every threshold is simulated independently

from the others, small-order relation problems (i.e., increasing threshold values do not correspond to nondecreasing indicator values) can occur. These have to be corrected before constructing a continuous CCDF, and we used the upward/downward correction procedure described by Goovaerts (1997, p. 324) for this. Because of the discontinuous nature of indicator coding, interpolation and/or extrapolation between and outside the threshold values has to be applied. This interpolation was done by a linear interpolation between threshold values, whereas for the lower tail extrapolation a power model was used and for the upper tail a hyperbolic one was used (Goovaerts 1997, p. 279). Finally, the CCDF was utilized to determine the expected value or probability of exceeding a critical threshold, as with SGS.

There are limitations to this indicator approach. It involves modeling as many variograms as there are thresholds, and it cannot use the full information in the original data. Information is lost by discretizing the continuous distribution of the data using a few thresholds. These, in turn, cause postprocessing problems where artificial choices have to be made to compensate for them, like the interpolation/extrapolation options.

Results and discussion

Exploratory data analysis

Our initial data comprised 14,674 Cu and 12,441 Cd observations of the top 0.5 m of the soil of Flanders (Fig. 1a and b). However, the density of available samples was uneven, especially near larger industrialized centers, such as the city of Antwerp (Fig. 1c), where many observations occurred in a clustered configuration.

Because the general objective of the data collection was to identify soil contamination, a bias in the sample statistics due to preferential sampling in areas of large concentrations was unavoidable. To remove this bias, first the extreme values were identified as outliers and excluded (Meklit et al. 2009), and second the observations retained were subjected to a cell-declustering procedure (Deutsch and Journel 1998).

To detect outliers in the data, breaks and inflections on the cumulative distribution plots have mainly been used (Reimann and Garrett 2005). However, this criterion summarizes only the global data distribution without making use of the local spatial distribution. It needs to be complemented, therefore, with information from the local spatial distribution (Lark 2002). This combination was analyzed and described by Meklit et al. (2009). According to the sample cumulative distribution function, values $> 9000 \text{ mg kg}^{-1}$ for Cu and $> 100 \text{ mg kg}^{-1}$ for Cd could be considered global outliers. These few values were evaluated in relation to their spatial neighbors and were also identified as spatial outliers, that is, local extreme values surrounded by small values (Meklit et al. 2009). Based on this analysis, data that could be considered outliers, both globally and spatially, were excluded. In this

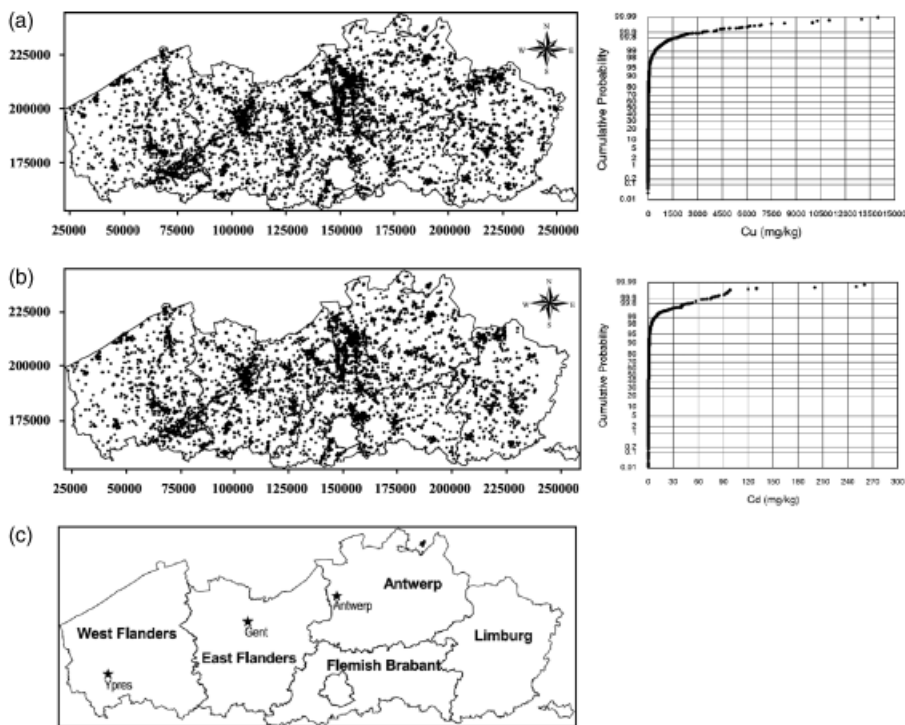


Figure 1. Location maps and sample cumulative distribution functions of topsoil (a) copper, (b) cadmium, and (c) the provinces of Flanders, Belgium, indicating the cities mentioned in the text. Coordinates are in meters according to the Belgian Lambert-72 projection.

way, 10 Cu and 11 Cd outliers were removed (representing 0.07% and 0.09% of the total data set, respectively).

The cell-declustering procedure (Deutsch and Journel 1998) consists of down-weighting clustered values and giving additional weight to isolated samples based on the number of observations within each cell. These weights were inversely related to the number of observations in a cell. The cell size was changed in a stepwise fashion until a minimum global mean was reached. Because an increase in the cell size further resulted in an increase in the mean, it was assumed that the cell size corresponding with the minimum mean represented the strongest removal of the bias. Therefore, the weights corresponding to this cell size were used as declustering weights. Declustering reduced the mean concentration of Cu from 58.2 to 35.4 mg kg⁻¹ and of Cd from 1.2 to 0.90 mg kg⁻¹ with clear reductions in the variances. The distributions before and after declustering are illustrated in Fig. 2. Declustering resulted in an increase in low values due to preferential sampling in areas where high metal concentrations would be expected.

The declustered distributions of the data of both heavy metals had a characteristic positively skewed shape with a wide range (Fig. 2); for example, 95% of the

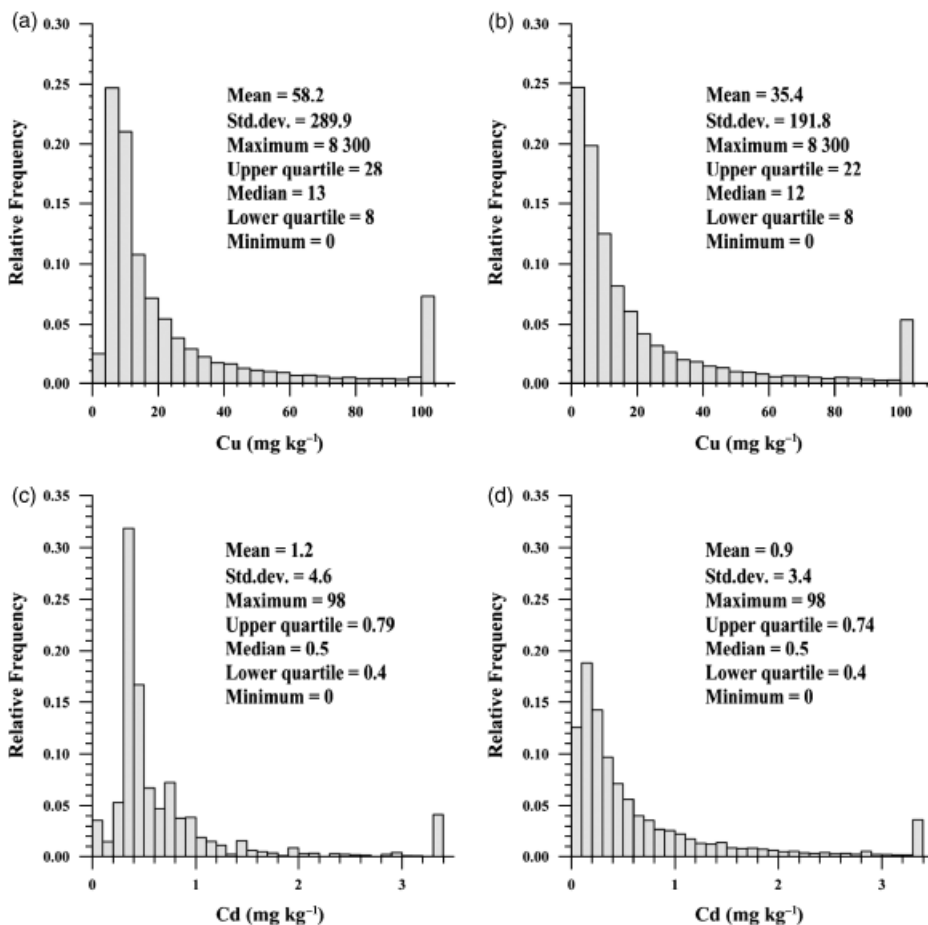


Figure 2. Histograms of topsoil data for copper: (a) without declustering and (b) after declustering; and for cadmium: (c) before declustering and (d) after declustering (data in the group of values represented by the last bar exceed the maximum of the X axis).

Cd measurements had values $<2.7 \text{ mg kg}^{-1}$, whereas the range extends from 0 to 98 mg kg^{-1} . Measured values of Cu extended from 0 to 8300 mg kg^{-1} , with 95% of them having values of $<90 \text{ mg kg}^{-1}$.

Cu

The 14,664 Cu observations retained were analyzed with SGS. As this procedure assumes a Gaussian distribution, the heavily skewed Cu data were subjected to a normal score transform. The histogram and the experimental and theoretical variograms of the normal scores are given in Fig. 3, together with the parameters of a nested variogram model composing a nugget effect and two exponential components. The nugget variance represents 39% of the sill variance ($0.45 \times 100/$

[0.45+0.28+0.41]), and 61% of the total variance is structured. Of this structured variance, 40% occurs within 452 m, whereas the rest occurs within 4279 m. This indicates that, apart from moderate noise or very short-range variation (the nugget variance), a considerable proportion of the variation in Cu shows a nested structure over spatial scales of several hundred meters (short-range component) to several kilometers (long-range component) within Flanders.

Using the variogram parameters and the normal score values, 500 realizations were generated for every estimation location (Chilès and Delfiner 1999, p. 453, recommended 100 realizations as a minimum). After postsimulation processing of the 500 realizations generated with SGS, the estimated values (equation [2]) and the probability of exceeding the critical sanitation threshold (equation [3]) were derived (Fig. 4). The Flemish reference sanitation threshold for agricultural land of 200 mg Cu kg⁻¹ was used as the critical threshold value, because it represents the worst-case scenario, that is, plants growing on such land or animals grazing on it, will produce products intended to be consumed by human beings.

Most of the soil of Flanders was estimated to have a Cu concentration between the background value of 17 mg kg⁻¹ and the sanitation threshold value of 200 mg kg⁻¹. Some patches have values below 17 mg kg⁻¹, but there are larger areas with estimated concentrations above 200 mg kg⁻¹. Most of the latter areas are associated with known industrial activities in areas, such as south of Antwerp, around Gent (Fig. 1c), and near to the border with the Netherlands in the northeast. One remarkable exception is in the south of the province of West-Flanders, around the city of Ypres (Fig. 1c). Here, Van Meirvenne et al. (2008) identified the First World War as the source of Cu, an essential element in the millions of shells fired during this war. The map shows that the probability of exceeding the critical sanitation threshold of 200 mg kg⁻¹ in the topsoil is below 25% for almost the

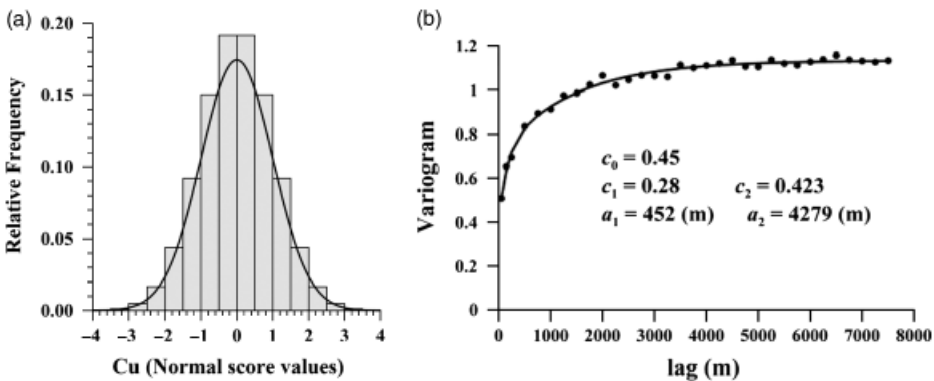


Figure 3. (a) Histogram of the normal score values of topsoil Cu with corresponding normal distribution and (b) the variogram of the normal score values fitted with a double exponential model—the parameters refer to a nested model with a nugget variance (Cd) plus two spherical models (equation [2]).

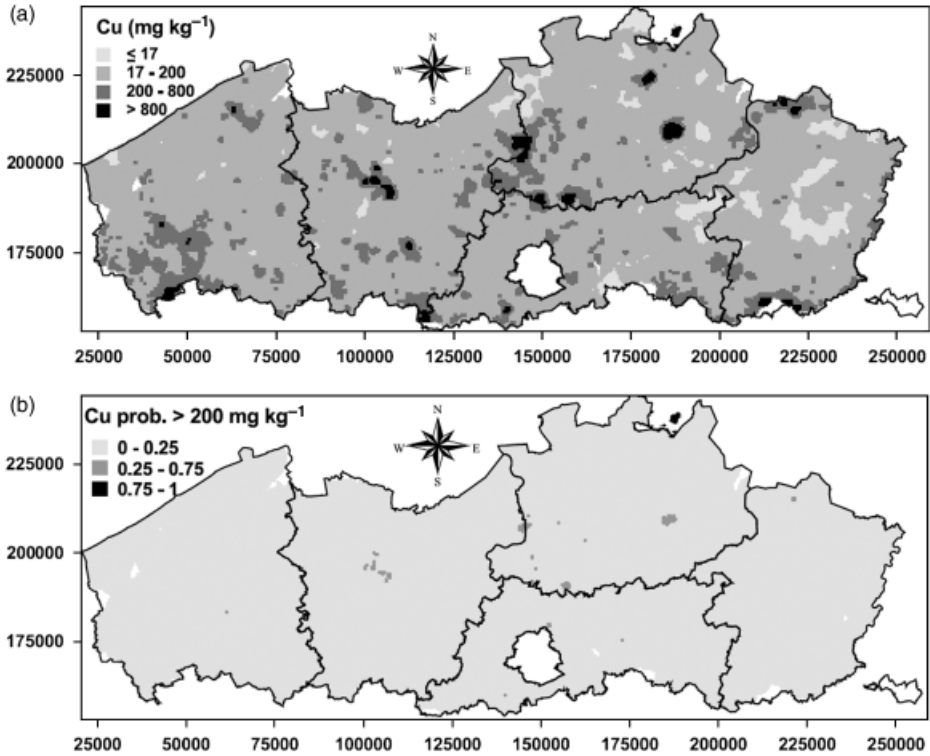


Figure 4. (a) Estimated values of topsoil Cu classified according to limits of the Flemish soil sanitation decree (b) and classified probability of exceeding the Cu sanitation limit for agricultural land use (200 mg kg^{-1}). Boundaries represent the Flemish provinces of Belgium.

entire study area. All areas with a 0.25–0.75 probability can be associated with known intensive industrial activities. In these areas, we suggest that the status of Cu should be examined further by additional sampling. No areas were identified where the probability level of exceeding the critical Cu threshold was above 0.75.

Cd

In contrast to Cu, the Cd data have many observations (43%) with values at or below the analytical detection limit of 0.4 mg kg^{-1} , and 30% of the data have values equal to 0.4 mg kg^{-1} (the data received were rounded to one decimal place) (Fig. 2c and d). This large number of equal values makes the normal score transformation problematic because of the need for a ranking sequence. Under such circumstances, the indicator approach offers an alternative.

The Cd data were first discretized using $K = 10$ thresholds z_k spanning most of the global declustered distribution ($z_k = 0.4, 0.5, 0.6, 0.7, 0.8, 0.9, 1.0, 1.3, 1.6, 2.0 \text{ mg kg}^{-1}$; Table 1). Ten variograms were calculated and modeled, one for each threshold, after coding the data as indicators (equation [4]). Fig. 5 shows the va-

Table 1. The 10 Indicator Threshold Values (z_k) Used to Discretized the Cadmium Data, the Proportion of Data Below This Threshold, and the Parameters of the Fitted Indicator Variograms (Double Spherical Models)

z_k (mg kg^{-1})	% data $\leq z_k$	c_0	c_1	a_1 (m)	c_2	a_2 (m)
0.4	43	0.43	0.46	555	0.07	4680
0.5	60	0.52	0.37	697	0.09	5002
0.6	66	0.56	0.33	643	0.10	4700
0.7	75	0.60	0.27	413	0.14	4697
0.8	78	0.67	0.21	509	0.17	4971
0.9	82	0.71	0.19	654	0.16	4320
1.0	86	0.83	0.26	2024	0.01	3361
1.3	90	0.87	0.26	2440	0.05	3373
1.6	92	0.89	0.19	2440	0.10	3373
2.0	94	0.94	0.1	2439	0.18	3373

Note: c_0 , nugget variance; c_1 and a_1 , structured variance and range of the first spherical model, respectively; c_2 and a_2 , the structured variance and the range of the second spherical model, respectively.

riograms, and Table 1 gives the parameters of the fitted nested models (double spherical models); they show that, as the Cd threshold increases, the nugget effect becomes increasingly dominant. For thresholds >0.8 , the first range structure increases and the second range one reduces. This indicates that small Cd values are more spatially continuous, whereas larger ones are more isolated spatially.

SIS provided 500 realizations of topsoil Cd and similarly of topsoil Cu; the estimated values (equation [2]) and the probability of exceeding the critical sanitation threshold (equation [3]) were obtained and mapped (Fig. 6). A critical sanitation threshold of 2 mg kg^{-1} was used, which is the Flemish reference sanitation threshold for agricultural land.

The estimated Cd remained below the background value of 0.8 mg kg^{-1} for most of the study area. Higher predicted concentrations were found in areas with extensive industrial activities, which is similar to the large estimates of Cu. However, the map indicates more areas with a probability between 0.25 and 0.75 than on the Cu map. There were even two patches with a probability of ≥ 0.75 of exceeding the critical threshold of 2 mg kg^{-1} : one south of Antwerp and one in the north of the province of Limburg (most eastern province; Fig. 1c). The site in Antwerp is associated with the historical activities of a lead factory, where heavy metal emissions have been measured. The second area (covering an area of 36.3 km^2) suffered from severe Cd contamination from emissions from several zinc smelters clustered in northern Limburg and the southern Netherlands. The Belgian part of this area was investigated in more depth by Van Meirvenne and Goovaerts (2001).

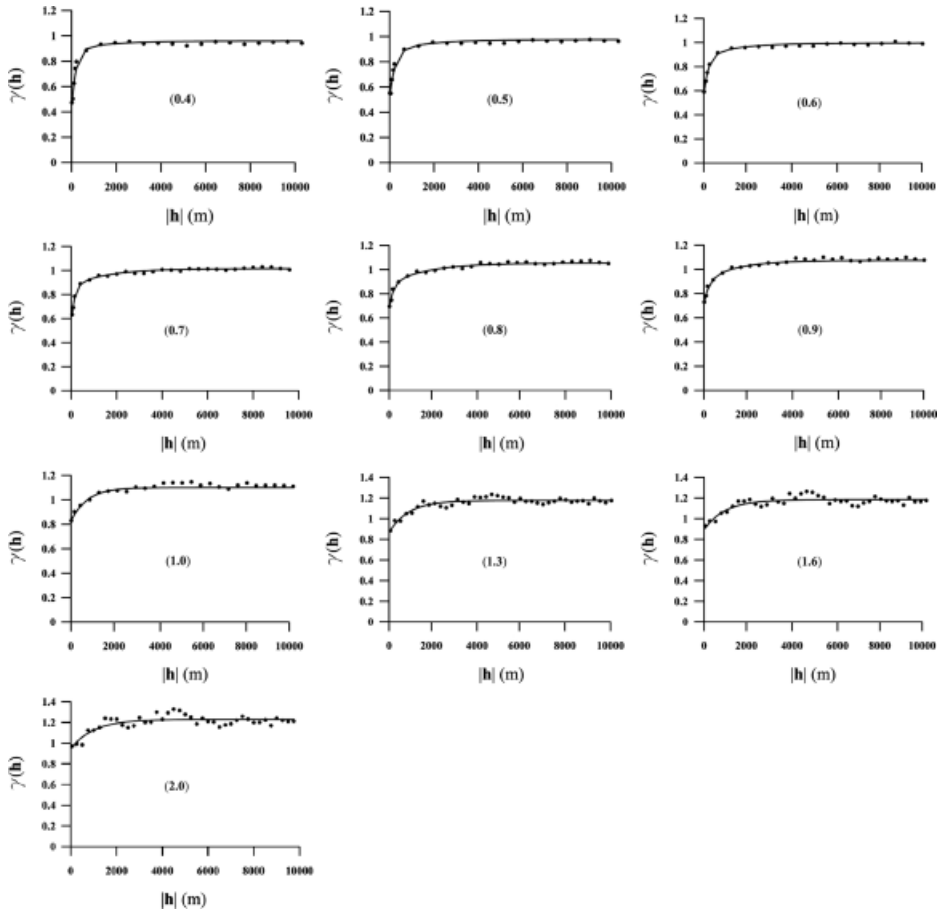


Figure 5. Indicator variograms of Cd (fitted double spherical models) for the 10 threshold values (in brackets) used in sequential indicator simulation.

Conclusion

The Cu data distribution was strongly positively skewed, and a normal score transformation was needed to make it Gaussian. The fitted nested variogram model indicated that, besides a moderate level of noise or variation over short distances, a considerable proportion of the variation in Cu was structured over spatial scales of several hundred meters to several kilometers.

Most of the study area was estimated to have a Cu concentration between the background value of 17 mg kg^{-1} and a reference sanitation threshold value of 200 mg kg^{-1} . In addition, most of the areas with an estimated probability of exceeding the reference critical sanitation threshold of 200 mg kg^{-1} between 0.25 and 0.75 could be associated with known industrial activities. In the south

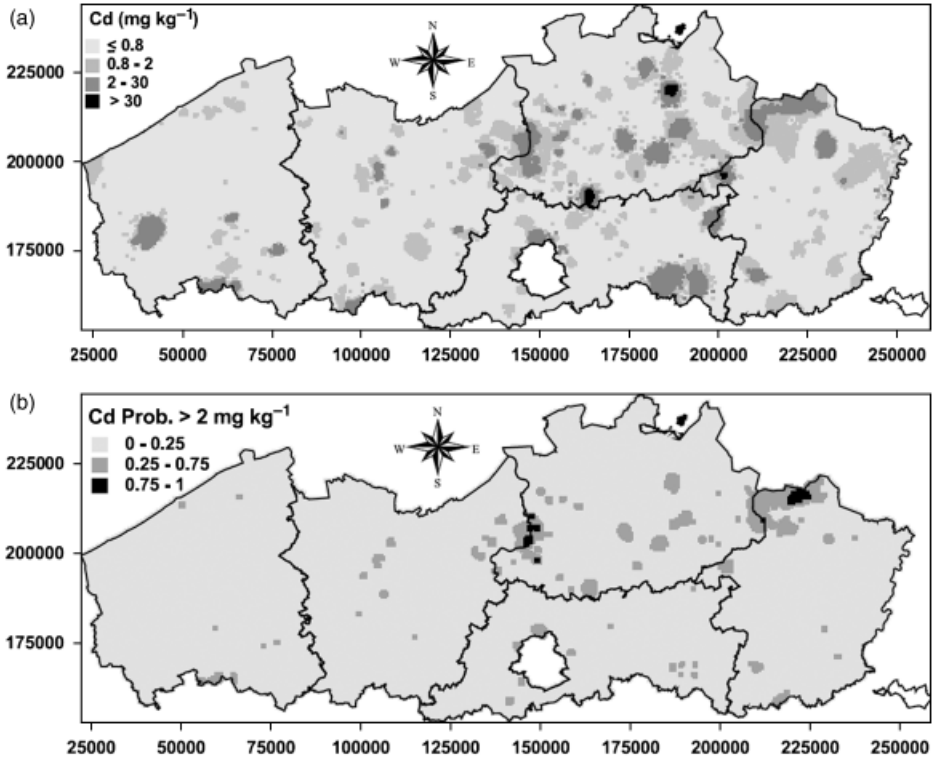


Figure 6. (a) Estimated values of topsoil Cd classified according to limits of the Flemish soil sanitation decree and (b) classified probability of exceeding the Cu sanitation limit for agricultural land use (2 mg kg^{-1}). Boundaries represent the Flemish provinces of Belgium.

of West-Flanders, a large area with increased Cu concentrations was identified as being related to shelling during the First World War.

Double spherical models fit the experimental variograms of these indicators best. They showed that small Cd values were more spatially continuous, whereas larger values were more isolated.

The estimated Cd remained below the background value of 0.8 mg kg^{-1} for most of the study area. However, the probability map indicates more areas with a probability of exceeding the critical threshold of 2 mg kg^{-1} between 0.25 and 0.75 than it does for Cu. There are even two patches with a probability of ≥ 0.75 of exceeding this threshold. Both could be related to known industrial environmental contamination.

Whereas most studies concentrate on a local scale on one or a few punctual sources of pollution, we have shown that geostatistical methods can also be used to analyze large data sets of regional data on soil heavy metals originating from a combination of diffuse and multiple punctual sources. For this purpose, we used SGS and SIS, which we found to be flexible methods.

Acknowledgement

We thank Public Waste Agency of Flanders (OVAM) for providing the data on heavy metals in the soil of Flanders that were used in this study.

References

- Chilès, J. P., and P. Delfiner. (1999). *Geostatistics Modelling Spatial Uncertainty*. New York: Wiley.
- Christakos, G. (2000). *Modern Spatiotemporal Geostatistics*. Oxford, UK: Oxford University Press.
- De Temmerman, L., L. Vanongeval, W. Boon, M. Hoenig, and M. Geypens. (2003). "Heavy Metal Content of Arable Soils in Northern Belgium." *Water, Air, and Soil Pollution* 148, 61–76.
- Deutsch, C. V., and A. G. Journel. (1998). *GSLIB: Geostatistical Software Library and User's Guide*, 2nd ed. New York: Oxford University Press.
- Fagroud, M., and M. Van Meirvenne. (2002). "Accounting for Soil Spatial Autocorrelation in the Design of Experimental Trials." *Soil Science Society of America Journal* 66, 1134–42.
- Goovaerts, P. (1997). *Geostatistics for Natural Resources Evaluation*. New York: Oxford University Press.
- Goovaerts, P. (2000). "Estimation or Simulation of Soil Properties? An Optimization Problem with Conflicting Criteria." *Geoderma* 98, 165–86.
- Goovaerts, P. (2001). "Geostatistical Modelling of Uncertainty in Soil Science." *Geoderma* 103, 3–26.
- Goovaerts, P., R. Webster, and J. P. Dubois. (1997). "Assessing the Risk of Soil Contamination in the Swiss Jura Using Indicator Geostatistics." *Environmental and Ecological Statistics* 4, 31–48.
- Lark, R. M. (2002). "Modeling Complex Soil Properties as Contaminated Regionalized Variables." *Geoderma* 106, 173–90.
- Meklit, T., M. Van Meirvenne, S. Verstraete, J. Bonroy, and F. Tack. (2009). "Combining Marginal and Spatial Outlier Identification to Optimize the Mapping of the Regional Geochemical Baseline Concentration of Soil Heavy Metals." *Geoderma* 148, 413–20.
- Papritz, A., C. Herzig, F. Bore, and R. Bono. (2005). "Modelling the Spatial Distribution of Copper in the Soils Around a Metal Smelter in Northwestern Switzerland." In *Geostatistics for Environmental Applications*, 343–54, edited by P. Renard, H. Demougeot-Renard, and R. Froidevaux. New York: Springer-Verlag.
- Rawlins, B. G., R. M. Lark, R. Webster, and K. E. O'Donnell. (2006). "The Use of Soil Survey Data to Determine the Magnitude and Extent of Historic Metal Deposition Related to Atmospheric Smelter Emissions Across Humberside, UK." *Environmental Pollution* 143, 416–26.
- Rawlins, B. G., R. Webster, and T. R. Lister. (2003). "The Influence of Parent Material on Topsoil Geochemistry in Eastern England." *Earth Surface Processes and Landforms* 28, 1389–409.
- Reimann, C., and R. G. Garrett. (2005). "Geochemical Background—Concept and Reality." *Science of the Total Environment* 350, 12–27.

- Salminen, R., M. Bidovec, M. J. Batista, A. Demetriades, B. De Vivo, W. De Vos et al. (2005). "Geochemical Atlas of Europe. Part 1: Background Information, Methodology and Maps. Geological Survey of Finland, Espoo." Available at <http://www.gtk.fi/publ/foregsatlas> (accessed June 22, 2007).
- Van Meirvenne, M., and P. Goovaerts. (2001). "Evaluating the Probability of Exceeding a Site-Specific Soil Cadmium Contamination Threshold." *Geoderma* 102, 75–100.
- Van Meirvenne, M., T. Meklit, S. Verstraete, M. De Boever, and F. Tack. (2008). "Could Shelling in the First World War Have Increased Copper Concentrations in the Soil Around Ypres?" *European Journal of Soil Science* 59, 372–79.
- Van Meirvenne, M., and I. Van Cleemput. (2005). "Pedometrical Techniques for Soil Texture Mapping at a Regional Scale." In *Environmental Soil-Landscape Modeling*, 323–41, edited by S. Grunwald.. Boca Raton, FL: CRC Press, Taylor & Francis Group.
- Vlaamse-Gemeenschap. (1996) "Besluit van de Vlaamse regering houdende vaststelling van het Vlaams reglement betreffende de bodemsanering." *Belgisch Staatsblad* # 27-3-1996.
- Webster, R., and M. A. Oliver. (2007). *Geostatistics for Environmental Scientists*, 2nd ed. Chichester, UK: Wiley.
- Zhang, C. S., F. T. Manheim, J. Hinde, and J. N. Grossman. (2005). "Statistical Characterization of a Large Geochemical Database and Effect of Sample Size." *Applied Geochemistry* 20, 1857–74.